Applied Physics Letters ARTICLE scitation.org/journal/apl

Subtractive patterning: High-resolution electrohydrodynamic jet printing with solvents

Cite as: Appl. Phys. Lett. **117**, 133702 (2020); doi: 10.1063/5.0021038
Submitted: 7 July 2020 · Accepted: 22 September 2020 ·
Published Online: 30 September 2020

Nazanin Farjam, Tae H. Cho, Neil P. Dasgupta, and Kira Barton[a)]

AFFILIATIONS

Department of Mechanical Engineering, University of Michigan, 2350 Hayward Ave., Ann Arbor, Michigan 48109, USA

[a)]Author to whom correspondence should be addressed: bartonkl@umich.edu

ABSTRACT

Advancements in 3D printing have initiated a paradigm in device fabrication. Electrohydrodynamic jet (e-jet) printing is a high-resolution 3D printing method that enables customizable patterning of thin-film structures, while reducing fabrication complexity and achieving high-resolution patterns with a wide variety of materials. However, to date, e-jet printing has focused on additive material deposition, rather than patterning through material subtraction. This work proposes displacement-based e-jet printing using solvent inks for subtractive patterning of polymer thin films, with microscale resolution in the x–y plane and nanoscale control in the z (dissolving) direction. The behavior of displacement-based e-jet printing is characterized using atomic force microscopy, and two methodologies are developed for controlling the linewidth and displaced depth. An example of area-selective thin film deposition on displacement-based e-jet patterns is provided to demonstrate the applicability of this patterning technique for printable microscale devices.

Interest in 3D printing of microelectronics as an alternative to standard photolithography methods has been gaining momentum due to unique advantages offered by printing processes, including (1) reduction in the number of fabrication steps; (2) flexibility to manufacture outside of a clean-room environment, which has the potential to lower costs; (3) ability to customize device architectures for applications such as personalized health care;[1] and (4) compatibility with curved and flexible substrates.[2–5]

Ink-jet printing has been demonstrated for use in direct printing of functional or structural inks.[6] However, the extension of ink-jet printing into the printed electronics market has been limited by restrictions in printed material selection due to tight tolerances in the viscosity and environmental control, as well as the relatively low resolution (>30 μm)[7] fabrication capabilities.

Electrohydrodynamic jet (e-jet) printing is a high resolution printing technique, 0.05–50 μm (Ref. 8) depending on printing conditions (e.g., nozzle size and applied voltage) and material properties (e.g., ink particle size, viscosity, and cohesion), which is capable of material ejection with a wide range of inks (viscous polymers, organics, inorganics, and conductive nanoparticle suspensions).[2,9] The working principle of e-jet printing involves the application of an electric field between a conductive nozzle and the substrate. This pulls ink material out of a nozzle into a conical shape known as a Taylor cone [Fig. 1(a)]. Charge build-up in the meniscus leads to material ejection at the tip, resulting in high resolution patterning, and the ability to print a wide variety of ink viscosity, ranging from 10^0–10^5 centipoise.

Despite the demonstrated range of e-jet applications,[2,10,11] this additive manufacturing technique has not been used for material subtraction, which would open up new applications in electronic device fabrication. For example, lithographic patterning of polymer films is an important step in many additive and subtractive processes, where several deposition and etching steps are patterned by lithographic masks that define the material pattern in the x–y plane. As an alternative, if e-jet printing with solvents can enable patterning of polymer thin films, the active areas for subsequent material deposition can be defined and used for processes ranging from lift-off to area-selective deposition. Compared to the existing techniques such as lithographic patterning, additive manufacturing provides advantages in design flexibility, rapid prototyping, and customizability within a given layer.[12]

In this work, we demonstrate an approach for subtractive patterning with e-jet printing. Termed displacement-based e-jet printing, a solvent ink is used to break down a polymer thin film and displace the polymer particles toward the boundary of the deposited droplet before evaporating, creating sub-15 μm linewidth patterns within the polymer films [Figs. 1(b)–1(d)]. Subtractive e-jet patterning has not been reported in the literature, and when compared to other 3D printing techniques such as direct laser writing,[13,14] displacement-based

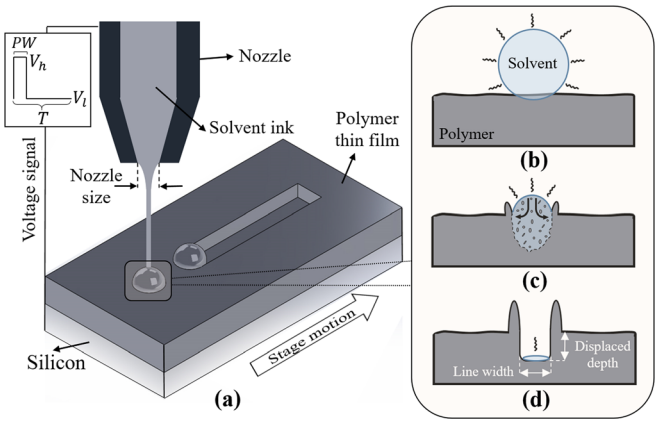

FIG. 1. Graphical description of the displacement-based e-jet printing process. (a) A printed solvent droplet comes into contact with the surface and (b) begins dissolving/pushing the polymer film in an outward flow while evaporating. (c) Finally, the polymer is completely displaced to the droplet boundaries.

e-jet printing provides advantages in terms of line speed and lower cost.[12,15]

To fully leverage the capabilities of this technique, we experimentally characterize the patterns achieved by displacement-based e-jet printing as a function of process parameters and experimental design.

Patterns created using e-jet printing are the result of three aspects of the printing process: droplet ejection, droplet spread on the substrate, and ink interactions with the substrate, which could be coalescence behavior for additive inks or evaporation-driven behavior for solvent inks. The droplet volume is controlled by the user through process parameter selection (e.g., pulse width of the applied voltage signal). The spreading and coalescence of the printed droplets on the substrate are driven by a combination of properties[16] including surface energy, liquid surface tension, and conductivity of the ink/substrate materials. Pannier *et al.*[17] developed a model that predicts the spreading of e-jet printed droplets of polymer ink on silicon and glass substrates, as well as layers of printed polymers. However, the interactions between an ejected droplet of solvent ink and a polymer thin film lead to significantly different spreading dynamics during the dissolution process, which have not been previously studied.

In this study, we explore how the ejected material volume and the number of layers printed over a given line affect the linewidth and displaced depth during displacement-based e-jet printing [Fig. 1(d)]. Knowledge of these parameters enables a quantitative method for achieving a desired pattern. To investigate the effects of the process parameters on the resulting patterns, we designed two experiments aimed at controlling the linewidth and displaced depth as separate variables. The methodology for these studies includes material selection, identification of pre-printing conditions, process parameter selection, and experimental design. Experimental parameters are provided in the supplementary material.

Polymethyl methacrylate (PMMA) is selected as the spin-coated base material, and 1-methyl-2-pyrrolidone (NMP) is selected as the solvent ink for these experiments.

The first step in the process requires spin coating of a polymer thin film. Parameters for spin coating the PMMA base layer include (1) spinning time and speed to determine the thickness of the polymer film and (2) time and temperature for post-baking, which affect the rate of polymer dissolution in the printed solvent material.[18]

To enhance polymer dissolution, we introduce a UV Ozone (UVO) treatment after the post-baking step to break chemical bonds in the polymer chains. Parameters involved during UVO treatment are (1) exposure time and (2) shelf life. The exposure time determines the number of chemical bonds that have been broken within the polymer chain. The shelf life is the amount of time between the treatment and e-jet printing of the solvent material. By varying these values, we observed that a significant exposure time led to a large increase in surface energy, while an extended shelf life resulted in a significant decrease in surface energy.

Key e-jet process parameters used to control the droplet volume (e.g., pattern resolution and depth) include the nozzle size, pulse width (PW) of the applied voltage signal, jetting frequency ($1/T$), applied voltage (high V_h, low V_l), offset height, stage speed, and number of printed layers along the same pattern (Fig. 1). If the e-jet deposited volume is too small, the solvent will evaporate before it has sufficient time to dissolve PMMA, while if the volume is too large, the x–y pattern resolution will decrease. Sequential layers of printed solvent can be used to increase the pattern depth. In this work, nozzle size, jetting frequency, applied voltage, offset height, and stage speed were kept constant across the experiments, while the pulse width and number of layers were used to control the resolution and depth of the printed patterns.

Two sets of experiments were performed to investigate the effects of the layer number and pulse width on the displaced polymer depth and linewidth. The first experiment aimed to control the pattern depth by varying the number of sequentially printed layers of solvent ink along the same path. In the second set of experiments, the displaced material linewidth was controlled by varying the pulse width of the high voltage signal and, hence, the volume of deposited ink. To demonstrate the repeatability of the process, printed layer patterns were repeated and measured three times per pattern on the same substrate. Measurements of the displaced material profile were taken using an atomic force microscopy (AFM) scan at three different locations on each printed line.

Experimental parameters (provided in the supplementary material) were determined heuristically through preliminary studies. Spin coating and UVO parameters were designed to maximize polymer dissolution in the printed solvent, while constant jetting parameters were selected to achieve high-resolution patterns.

Parameter variations in the preliminary studies induced two modalities of solvent (NMP) interaction with the coated polymer (PMMA). The two distinct behaviors, illustrated in Fig. 2, demonstrate well-known droplet/surface interactions that have been demonstrated in previous droplet studies.[19–21]

The first behavior, termed a coffee ring effect, describes a process in which liquid evaporating along the edge of a droplet is replaced with liquid from the center of the droplet, which leads to fluid flow from the center toward the edges of the droplet[19] [Fig. 2(a)]. This process is driven by an evaporation rate gradient that exists along the droplet,[21] often resulting in rings of evaporation for a single droplet of printed ink.

In solvent-based e-jet printing of a pattern/line, the solvent initially breaks down the polymer base layer, resulting in thorough dissolution of the polymer in the solvent. Then, fluid flow occurs toward

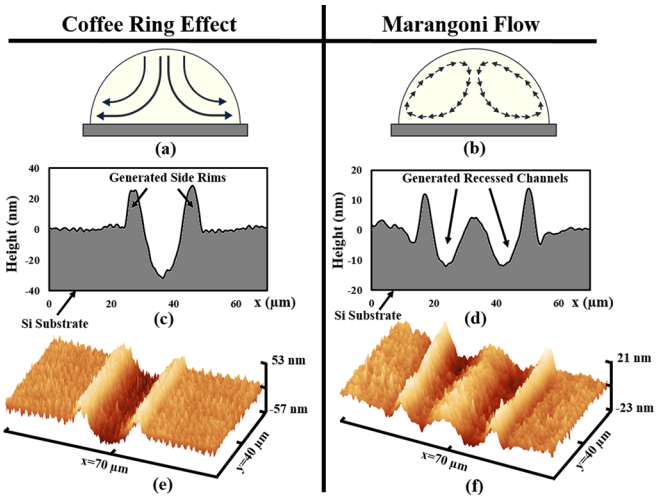

FIG. 2. Droplet interactions on a surface: (a) illustration of a "coffee ring effect." (b) Illustration of a "Marangoni effect." (c) Atomic force microscopy (AFM) 2D scan and (e) 3D scan showing a coffee ring effect in a displacement-based e-jet printed pattern. (d) AFM 2D scan and (f) 3D scan of a Marangoni flow-based printed pattern from displacement-based e-jet printing.

the edge of the line, due to a solvent evaporation gradient that forms along the width of the printed line. This fluid flow, containing the dissolved polymer, displaces the polymer toward the edge of the printed line as the solvent evaporates, leaving an accumulation of the solidified polymer along the edge of the channel and creating side rims. This process has also been observed in inkjet printing.[22] Figure 2(c) shows an AFM scan of a channel created by a coffee ring effect in a polymer thin film using solvent-based e-jet printing. The width and depth of the recessed channel [Fig. 2(c)] are controlled by the amount of material ejected in a single pass and the number of layers that are printed along the same path.

The second behavior, termed Marangoni flow, defines a process in which a non-uniform evaporation rate along a droplet causes a temperature gradient that leads to a surface-tension gradient along the droplet free surface [Fig. 2(b)]. The surface-tension gradient induces inward fluid flow from the free surface of the droplet toward the center of the droplet.[20,21]

When Marangoni flow is induced during solvent e-jet printing, a fluid flow is generated in a circular pattern from the edges of the deposited fluid toward the center of the printed pattern. This circular fluid flow displaces the locally dissolved polymer in the solvent ink from the edge of the pattern back toward the center of the pattern. This results in a large central line of the deposited polymer and two recessed side channels, as shown in the AFM scan of an e-jet patterned feature in Fig. 2(d).

Marangoni flow has been shown to result in uniform thin films when depositing materials coalesce together.[21] However, for displacement-based e-jet printing, where the ability to define and control the parameters of a single recessed pattern is desired, the generation of two side channels caused by Marangoni flow, as depicted in Fig. 2(d), reduces the repeatability and reliability of the created pattern. To ensure control during displacement-based patterning, the process parameters that induce a coffee ring effect were identified and kept constant throughout the experimental testing. Low jetting frequencies minimized the potential for solvent to flood an area, reducing the risk for Marangoni effects. Similarly, a short shelf life after UVO treatment (<24 h) maintained the UVO effects, which led to coffee ring rather than Marangoni flows.

To assess the effects of the printed layer number and pulse width on the displaced depth and linewidth of the resulting pattern, consider the experimental results illustrated in Fig. 4. In experiment 1, the number of printed layers of solvent material was varied from one to eighty, while holding all other parameters constant and selecting a pulse width of 30 μs. In experiment 2, the pulse width was varied from 30 μs to 40 μs, with the number of layers set to 10. The AFM top view images of the printed lines for experimental setups 1 and 2 are provided in Fig. 3 with a guide line to show the straightness of the created channels.

Figure 4 shows channel linewidth vs displaced depth as a function of layer number and pulse width length. Each measurement in Fig. 4 shows the mean and standard deviation of nine sample points around a nominal centerline, as demonstrated by the lines drawn onto the top view AFM images (see Fig. 3). It was observed that an increased layer number directly led to an increased displaced depth. An indirect consequence of printing multiple layers was an increase in the linewidth. For a PMMA layer thickness of 47 nm, approximately 40 layers of printed solvent material were required to displace all PMMA and expose the underlying silicon substrate. Forty printed layers resulted in an average linewidth of 12 μm. Increasing the number of layers beyond 40 layers led to small depth changes and relatively large linewidth changes.

To directly control the linewidth, consider the results from experiment 2 (Fig. 4). The increased pulse width resulted in an increased linewidth. In this experiment, the linewidth increased from an average of 6 μm to 17 μm over a 10 μs increase in the pulse width. Indirectly, the displaced depth also increased as a function of increasing pulse width. This is because a larger volume of deposited solvent material leads to more of the base material being dissolved and displaced. Here, increasing the pulse width resulted in an increase of 7 nm in the displaced depth, where the percent change in the displaced depth was significantly smaller than that observed upon increasing the number of layers. Therefore, the pulse width is determined to be an ineffective parameter to increase the displaced depth since it comes with a cost of significant loss in the x–y resolution. Evaluating the results in Fig. 4,

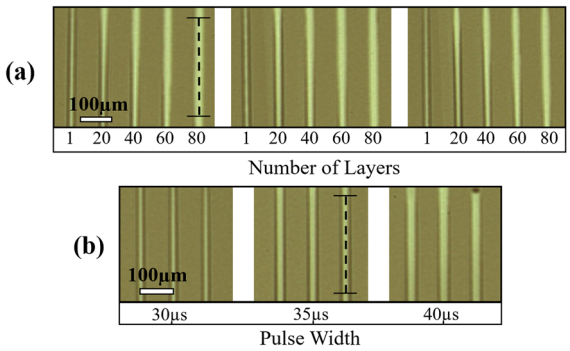

FIG. 3. AFM top view of printed lines. (a) Experiment 1: pulse width = 30 μs + varying layer number and (b) experiment 2: number of layers = 10 + varying pulse widths.

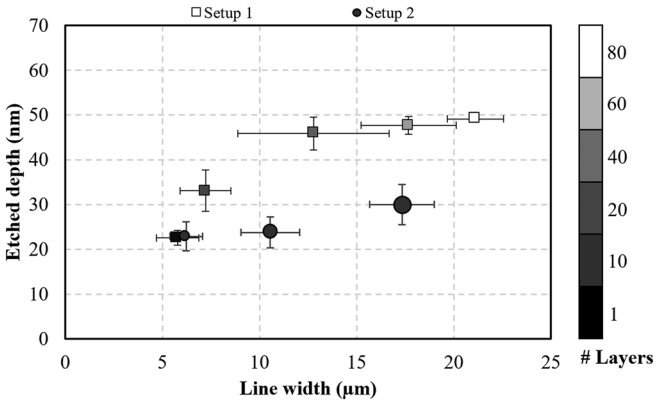

FIG. 4. Pattern resolution. AFM measurements of displaced depth vs linewidth. The color indicates the number of layers; the marker size indicates the pulse width length.

we observed that increasing the number of layers provides a more significant impact on the displacement-based patterning process. In particular, higher resolution (smaller line widths) and more densely packed patterns (see Sec. III in the supplementary material) can be achieved by increasing the number of layers applied to a given pattern. Alternatively, for a specified displaced depth, the most direct method for varying the linewidth is to increase the pulse width of the applied voltage. This can be used to design patterns with varying channel widths for applications in microfluidics, etc.

To demonstrate the effectiveness of the proposed approach, we conducted a case study combining solvent-based e-jet printing with area selective atomic layer deposition (AS-ALD). ALD is a thin-film deposition process that facilitates sub-nm control of thickness in the z direction through sequential exposure of the surface to self-limiting chemical reactions. While conventional ALD provides a uniform coating of the surface, changes to the surface chemistry of the substrate can enable selective suppression (or promotion) of the local deposition rate.[23–26] The channels resulting from the e-jet printed solvent provide an effective spatial (x–y) pattern for AS-ALD.

In this case study, zinc oxide (ZnO), a common semiconductor material, was selectively deposited on a silicon wafer (Si) in the e-jet displaced channels built within the PMMA base layer, see Fig. 5. Note that PMMA is a growth inhibitor for ZnO.[27] Patterns of deposited ZnO were demonstrated at a resolution of 10–15 μm. This case study

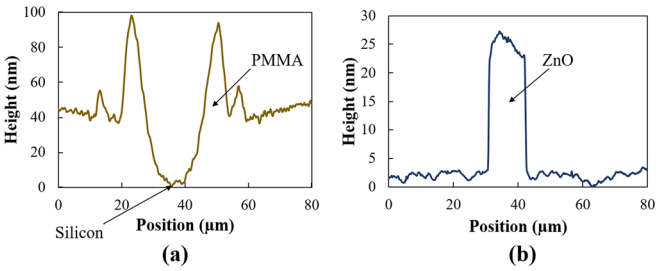

FIG. 5. Area-selective ALD example. (a) AFM scan of displacement-based channels after e-jet printing. (b) AFM scan of ALD fabricated ZnO.

demonstrates the effectiveness of displacement-based e-jet printing as an enabling technology in nanomanufacturing platforms. E-jet printing provides an alternative to traditional lithography processes for generating high-resolution patterns with reduced costs.

To summarize, solvent-based e-jet printing provides an approach for achieving flexibility in area-selective patterning with high resolution in the x–y plane and precise control in the z-axis. The parametric study presented in this work provides several key points of understanding related to the behavior of displacement-based e-jet printing as a function of process parameters. The results indicate that controlled patterning can be achieved by inducing coffee ring displacement of the polymer particles, while the desired depth and linewidth are derived through sequential printing across the same line known as the number of printed layers. In this first demonstration of displacement-based e-jet printing, we focused on understanding key properties of subtractive patterning with e-jet rather than optimizing the channel resolution or accuracy. In order to increase the resolution (ideally to sub-micrometers which is within the capability of e-jet in an additive printing mode) or improve the accuracy (minimizing the standard deviation observed in Fig. 4), both the pre-printing conditions (e.g., PMMA-deposited thickness and UVO exposure time) and printing parameters (e.g., nozzle size, applied voltage signal, and jetting frequency) need to be optimized. Potential applications for displacement-based e-jet printing range from microfluidics to printable electronics, which are enabled by this paradigm in subtractive printing at the nano-to-micro scale.

See the supplementary material for additional details on experimental setups, as well as more results including rim width control (Fig. S2) and study of the crossing lines (Fig. S3).

This work was supported by National Science Foundation Grant No. CMMI1727918.

DATA AVAILABILITY

The data that support the findings of this study are available within this article and its supplementary material.

REFERENCES

[1]A. Zucca, C. Cipriani, Sudha, S. Tarantino, D. Ricci, V. Mattoli, and F. Greco, Adv. Healthcare Mater. **4**, 983 (2015).
[2]M. S. Onses, E. Sutanto, P. M. Ferreira, A. G. Alleyne, and J. A. Rogers, Small **11**, 4237 (2015).
[3]M. Singh, H. M. Haverinen, P. Dhagat, and G. E. Jabbour, Adv. Mater. **22**, 673 (2010).
[4]J. R. Castrejon-Pita, W. R. S. Baxter, J. Morgan, S. Temple, G. D. Martin, and I. M. Hutchingsr, Atomization Sprays **23**, 541 (2013).
[5]E. Tekin, P. J. Smith, and U. S. Schubert, Soft Matter **4**, 703 (2008).
[6]M. Gao, L. Li, and Y. Song, J. Mater. Chem. C **5**, 2971 (2017).
[7]B. Derby, Annu. Rev. Mater. Res. **40**, 395 (2010).
[8]M. S. Onses, A. Ramrez-Hernandez, S.-M. Hur, E. Sutanto, L. Williamson, A. G. Alleyne, P. F. Nealey, J. J. de Pablo, and J. A. Rogers, ACS Nano **8**, 6606 (2014).
[9]J.-U. Park, M. Hardy, S. J. Kang, K. Barton, K. Adair, D. kishore Mukhopadhyay, C. Y. Lee, M. S. Strano, A. G. Alleyne, J. G. Georgiadis, P. M. Ferreira, and J. A. Rogers, Nat. Mater. **6**, 782 (2007).
[10]Y. Han and J. Dong, J. Micro- Nano-Manuf. **6**, 040802 (2018).
[11]B. H. Kim, M. S. Onses, J. B. Lim, S. Nam, N. Oh, H. Kim, K. J. Yu, J. W. Lee, J.-H. Kim, S.-K. Kang, C. H. Lee, J. Lee, J. H. Shin, N. H. Kim, C. Leal, M. Shim, and J. A. Rogers, Nano Lett. **15**, 969 (2015).

[12]D. Engstrom, B. Porter, M. Pacios, and H. Bhaskaran, J. Mater. Res. **29**, 1792 (2014).
[13]Y. Yu, Y. Deng, M. A. A. Hasan, Y. Bai, R.-Z. Li, S. Deng, P. Joshi, S. Shin, and A. Hu, Nanoscale Adv. **2**, 1195 (2020).
[14]A. Maurice, L. Bodelot, B. K. Tay, and B. Lebental, Small **14**, 1801348 (2018).
[15]A. Zhakeyev, P. Wang, L. Zhang, W. Shu, H. Wang, and J. Xuan, Adv. Sci. **4**, 1700187 (2017).
[16]C. P. Pannier, K. Barton, D. Hoelzle, and Z. Wang, *Dynamic Systems and Control Conference* (ASME, 2015).
[17]C. P. Pannier, M. Diagne, I. A. Spiegel, D. J. Hoelzle, and K. Barton, J. Manuf. Sci. Eng. **139**, 111008 (2017).
[18]D. Brambley, B. Martin, and P. D. Prewett, Adv. Mater. Opt. Electron. **4**, 55 (1994).
[19]R. D. Deegan, O. Bakajin, T. F. Dupont, G. Huber, S. R. Nagel, and T. A. Witten, Nature **389**, 827 (1997).
[20]H. Hu and R. G. Larson, J. Phys. Chem. B **110**, 7090 (2006).
[21]M. Majumder, C. S. Rendall, J. A. Eukel, J. Y. L. Wang, N. Behabtu, C. L. Pint, T.-Y. Liu, A. W. Orbaek, F. Mirri, J. Nam, A. R. Barron, R. H. Hauge, H. K. Schmidt, and M. Pasquali, J. Phys. Chem. B **116**, 6536 (2012).
[22]E. S. Park, Ph.D. thesis (University of California at Berkeley, 2013).
[23]D. Bobb-Semple, K. L. Nardi, N. Draeger, D. M. Hausmann, and S. F. Bent, Chem. Mater. **31**, 1635 (2019).
[24]K. J. Park, J. M. Doub, T. Gougousi, and G. N. Parsons, Appl. Phys. Lett. **86**, 051903 (2005).
[25]N. F. W. Thissen, R. H. J. Vervuurt, A. J. M. Mackus, J. J. L. Mulders, J.-W. Weber, W. M. M. Kessels, and A. A. Bol1, 2D Mater. **4**, 025046 (2017).
[26]E. Frm, M. Kemell, M. Ritala, and M. Leskel, J. Phys. Chem. C **112**, 15791 (2008).
[27]D. H. Levy, C. R. Ellinger, and S. F. Nelsonb, Appl. Phys. Lett. **103**, 043505 (2013).